PROGRESS IN THE RETRIEVAL OF SULPHUR SPECIES FROM MIPAS

A.B. Burgess, R.G. Grainger, and A. Dudhia

Atmospheric, Oceanic and Planetary Physics, Department of Physics, University of Oxford,
Oxford, OX1 3PU, UK
aburgess@atm.ox.ac.uk

ABSTRACT

Operationally only pressure, temperature and six significant trace gases are retrieved by ESA from MIPAS data. However, information on many other species is also present in the spectra. We apply a variety of techniques and our own retrieval model to retrieve the concentration of three other species: SO_2, OCS and SF_6. Sulphur Dioxide (SO_2) is an acidic gas with both natural and anthropogenic sources that is rapidly converted to sulphuric acid and hence sulphate aerosols in the atmosphere. Carbonyl Sulphide (OCS) is produced naturally at the ocean surface and by biomass burning and, through stratospheric oxidation, it is thought to be the main contributor to non-volcanic stratospheric sulphate aerosols. Sulphur Hexafluoride (SF_6) is almost entirely anthropogenic in its origins and shows steady year-on-year increases making it useful for age of air and tracer studies. We anticipate the good global coverage and continuity of data will make MIPAS useful for the determination of changes and trends in the quantity and distribution of these species – both natural and anthropogenic. In this paper we summarise the current progress that has been made in the retrieval of these important sulphur-containing species. We show some preliminary zonal mean fields and briefly outline the methods applied.

Key words: Envisat,MIPAS,OCS,SO2,SF6,Sulphur.

1. INTRODUCTION

The Michelson Interferometer for Passive Atmospheric Sounding (MIPAS) is one of the instruments aboard the European Space Agency's ENVISAT satellite. The sun-synchronous polar orbiting satellite has a period of one hundred minutes, giving approximately 14 orbits per day. MIPAS measures infrared atmospheric limb thermal emission spectra from 685–2410 cm^{-1}, which corresponds to a wavelength range of 14.5–4.1 μm. This range enables the remote monitoring of a wide variety of trace species. The nominal altitude range observed by MIPAS is is 6–68 km, covering the upper troposphere, the stratosphere and the lower mesosphere.

1.1. Carbonyl Sulphide

Carbonyl Sulphide, OCS, is relatively unreactive in the troposphere, so is available to enter the stratosphere in significant quantities. OCS is directly emitted from the oceans as a byproduct of both biological and photochemical reactions and has seasonally-varying source and sink terms from soils and forests [28, 30]. Anthropogenic activities, such as biomass burning and rice cultivation, add to the atmospheric OCS burden and aluminium production has also been highlighted as a previously unnoticed source [9, 25]. Recent analyses have shown deep convective events can transport large quantities of OCS through the tropical tropopause into the stratosphere [16]. Here it is susceptible to oxidation by hydroxyl radical attack and to ultraviolet photolysis [2]. OCS had been proposed as the major source of Stratospheric Sulphate Aerosols (SSAs) by Crutzen [6]. More recently, however, this almost exclusive assignment of the origin of SSAs to has come into question [4]. Large uncertainties in the atmospheric sulphur budget compound the problems associated with in situ measurement of background SSAs and makes an exact assessment of the OCS contribution extremely difficult [10, 25]. In fact, models suggest that under 50% of SSA particles originate from OCS, the remaining sources of sulphate being upward transport from the troposphere and SO_2 oxidation [17, 24]. A common observation by these authors, of special relevance to this work, is the scarcity of globally distributed profile information for both OCS and SO_2, making the validation of model predictions difficult. The solution to this problem is ideally suited to satellite measurements, with their global coverage.

1.2. Sulphur Dioxide

Sulphur Dioxide, SO_2, is an acidic gas with both natural and anthropogenic origins and is of interest to scientists due to its close links with aerosol formation and acidification of precipitation in the troposphere. SO_2 forms a major part of the sulphur cycle in the Earth's atmosphere. It is soluble in clouds and aerosol droplets, where is it able to react to form sulphuric acid, H_2SO_4. In general, the maximum concentration of SO_2 is close to its source

and the amount of SO_2 decreases rapidly with distance, indicative of a short tropospheric lifetime. In the dry stratosphere, especially at low altitudes where the concentration of OH radicals is small, the lifetime for SO_2 rises to the order of a few weeks [22, 26]. Direct injection of SO_2 into the stratosphere by volcanic activity results in the increased formation of stratospheric aerosols. Photolysis of H_2SO_4 aerosols leads to an increase in SO_2 in the upper stratosphere, [27].

1.3. Sulphur Hexafluoride

SF_6 is one of the most efficient greenhouse gases: it is three times stronger as a 'greenhouse gas' than an equivalent volume mixing ratio (VMR) of CFC–11 [11] and a thousand times that of CO_2. The contribution of SF_6 to radiative forcing is small because its current atmospheric concentration is less than five parts per trillion by volume (pptv) [14, 15, 20, 29]. The sources of SF_6 are almost entirely anthropogenic [11] although traces may originate naturally from fluoritic rocks [8]. There is evidence that the atmospheric concentration of SF_6 is increasing by about 7–8% per year [15, 19]. However, it has been suggested that the rate of increase in emission, if not production, has slowed in the past few years [5, 13]. Recent work [3] in applying MIPAS measurements to SF_6 led to a stratospheric growth rate for October 2002 to 2003 of 6.5±1.3 % yr^{-1} and a VMR for October 2003 of 4.60±0.05 pptv. This is within the envelope of forecasts from previous studies, but supports the suggestion that the rate of emission is decreasing. The well known emission record of SF_6 combined with its chemical inertness make it an ideal candidate for use as a tracer and for age of air calculation. Hence, it is useful in determining the flux of other species into the stratosphere.

Overall, the major anthropogenic sulphur-containing gas emissions are in the form of SO_2, whereas the dominant biogenic emissions consist of (mainly oceanic) DiMethyl Sulphide [4, 22] and CS_2 [25]. However, due to its lifetime OCS is thought to account for more than 80% of gas phase sulphur in the upper troposphere [16]. Sulphur hexafluoride may be considered as wholly inert over the altitude of interest, and as such forms an excellent tracer species.

2. RETRIEVAL METHODOLOGY

As with all species targeted for retrieval from MIPAS, an initial feasibility study was performed. This gives a good indication of the benefit that will be obtained by further study of the species. Firstly, a reference climatology profile [18] that forms a part of the MIPAS processing dataset was used to simulate the radiance contribution from the target species expected at the satellite. This is shown for OCS in Figure 1. There is no latitudinal or seasonal variation in any of the three species for the reference climatology, so all retrieved latitudinal structure is based on the effect of measurements. Figure 2 shows the simulated radiance and contribution of the sulphur species for a 12 km tangent height, with the instrumental noise levels (NESR)

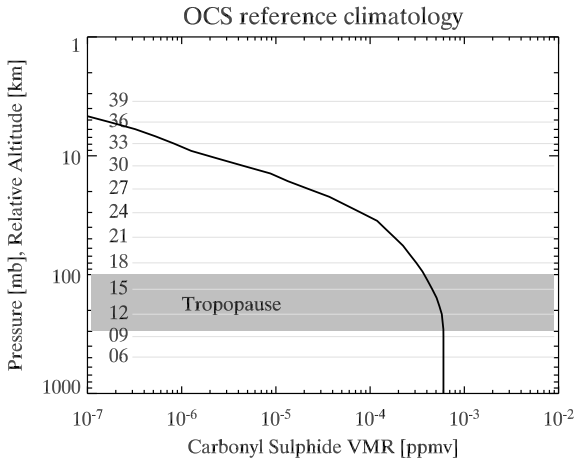

Figure 1. Carbonyl sulphide climatology, initially used in the study of retrieval feasibility.

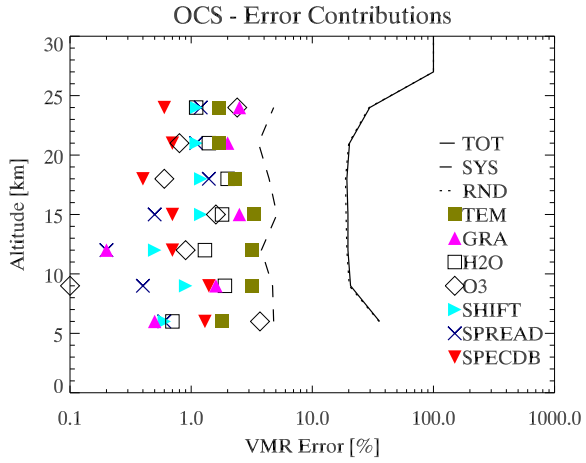

Figure 3. Assignment of various error sources to the final error budget as calculated during microwindow selection. The total error is shown (solid line) together with the random error component (dotted line) based on the instrument NESR. The total of the systematic error contributions is also shown (dashed line). Significant systematic error sources include: 'TEM' – retrieved temperature uncertainty, 'GRA' – error from a horizontal temperature gradient, 'H2O' – water vapour uncertainty, 'O3' – ozone profile uncertainty, 'SHIFT' – error from spectral calibration, 'SPREAD' – uncertainty in the ILS and 'SPECDB' – uncertainty in spectroscopic line parameters. The a priori error is assumed to be 100%.

shown per band. OCS is unusual amongst species that emit within the MIPAS spectral range as it exhibits its most significant emission in band 'D', between 1850 and 2410 cm^{-1}, so is the only species whose primary retrieval information originates in this band.

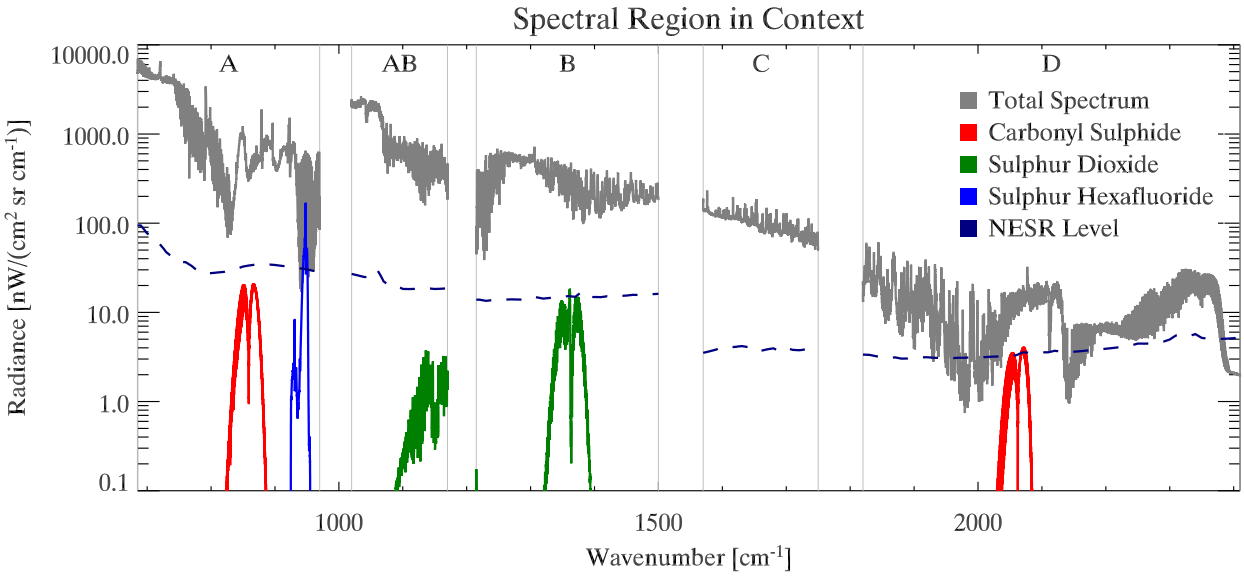

Figure 2. A radiative transfer simulation of the relative intensity of the sulphur species features compared to the total radiance for a 12 km tangent altitude, based on climatological abundances. The instrument noise level (NESR) is shown as the dashed horizontal line.

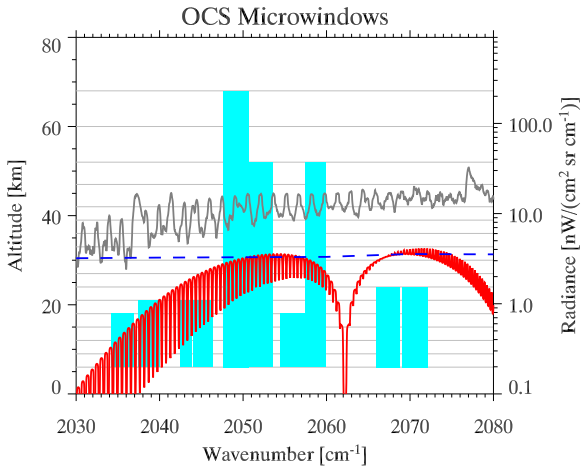

Figure 4. Plot indicating the position and altitude range (shaded blocks, left axis) of the selected microwindows, overplotted with the total radiance (grey line, right axis) within the significant spectral region for a 12 km tangent height. The lowermost red line (right axis) shows the radiance contribution from OCS to this total radiance. The MIPAS nominal measurement altitudes are shown as pale horizontal lines.

2.1. Microwindows

The selection of microwindows enabled a more detailed consideration of the feasibility of retrieval. Microwindows are small regions of the spectrum no more than 3 cm^{-1} wide. These regions are optimised to maximise the information obtained on the target species, whilst minimising both random and systematic errors. An informative discussion of the development of the microwindow selection algorithm may be found in Dudhia et al. [7] and an updated version is available in these proceedings. Together with the microwindow regions, a detailed error analysis is also obtained, showing the relative significance of all the known error sources. Again, OCS is used as an example, although the same procedure and error analyses exist for the other species. The error analysis is shown in Figure 3. As a result of the analysis, we can conclude that the range over which an OCS retrieval should be worthwhile is 6–25 km, with 30 km as an upper limit. The microwindow spectral and altitude ranges are shown in Figure 4. Similar results were obtained for the other species. The microwindow selection was validated using controlled retrievals from 'blind test' spectra, originally created as part of the E.U. Framework V 'AMIL2DA' study [1].

In order to perform the retrievals, we focused on an optimal estimation approach, formalised by Rodgers [21]. In addition a simple cloud-screening procedure, based on the ratio of two small spectral regions [23] was also applied. This removed those scans containing cloud. On completion, tests are performed on the diagnostics of the retrieval to remove any profiles are physically unreasonable. Use of the averaging kernels allows us to check both the amount and the vertical distribution of information in the final result that has been contributed by the measurement.

3. RESULTS

The results are grouped into three sections, by species.

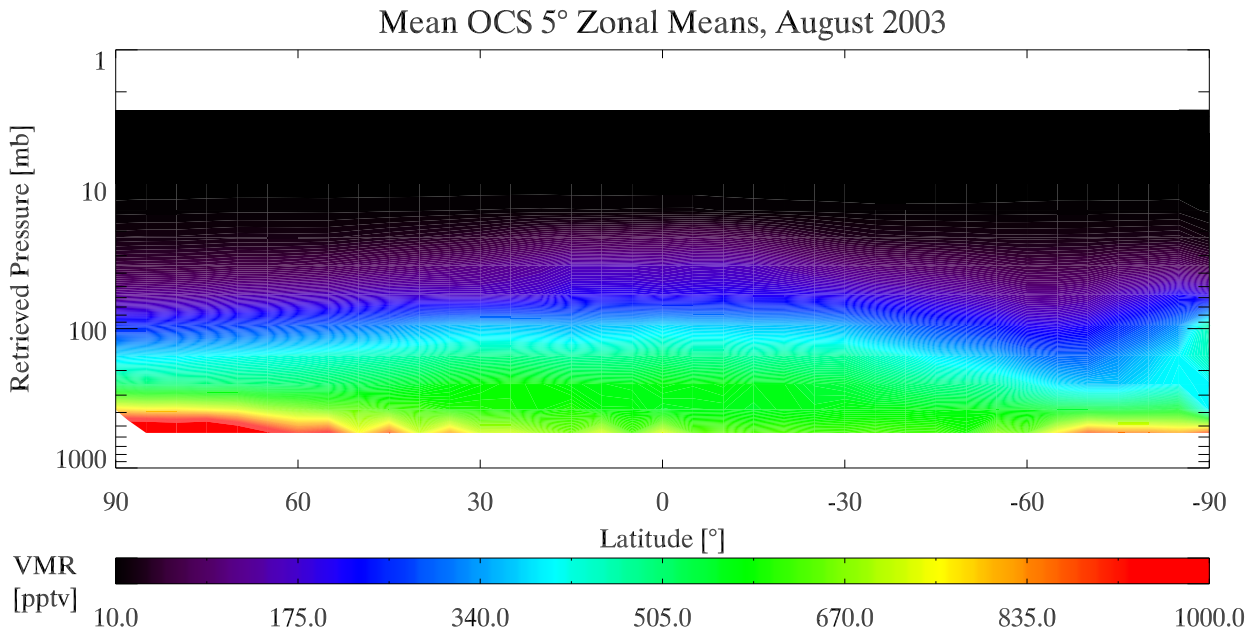

Figure 6. Zonal mean OCS distribution, August 2003. Approximately 10,000 retrieved values were binned to a 5° latitude by 3 km altitude grid covering the globe. For each bin large statistical outliers, if present, were removed. Note the higher values over the Northern latitudes at low altitude (6 km), possibly due to anthropogenic emissions. The low values recorded in a band around 70S may be due to a mixture of dynamical and (photo-)chemical processes – there are observed correlations with both the vortex range and terminator – but the low polar winter temperatures coupled with the location of the microwindows in the 'D' band (on the tail of the Plack curve) may be significant. Correlative data for validation is lacking so this is an area for further investigation. Although not shown in this figure, high variability was observed in the southern polar region, probably originating from the fact that the mean is computed from measurements that are both inside and outside the vortex.

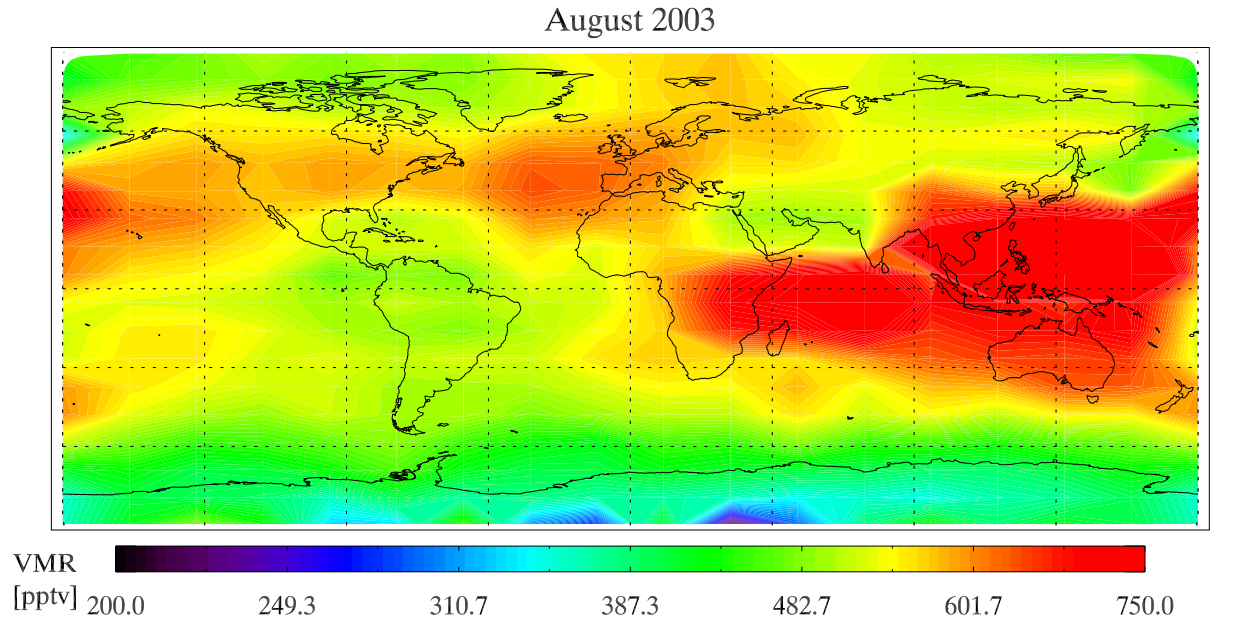

Figure 7. A 'slice' through Figure 6 showing the global distribution of OCS between 11 and 13 km (150 to 250 mb). Approximately 10,000 retrieved values were binned to a 20° by 10° grid covering the globe. For each bin large statistical outliers, if present, were removed. The high values over Indonesia may be anomalous, as there is very poor coverage in this region (dynamical effects cause strong ascent in this region, leading to almost all profiles being invalidated by cloud). However, the values are consistent out into the Indian Ocean, which has much more acceptable coverage. In addition, the structure over the Northern Atlantic and Europe is not unreasonable. The lower values (around 300 pptv – blue) centered over the southern winter pole are indicative of descending air from around 15 to 20 km as the main OCS loss mechanisms, such photolysis, do not operate in the polar night.

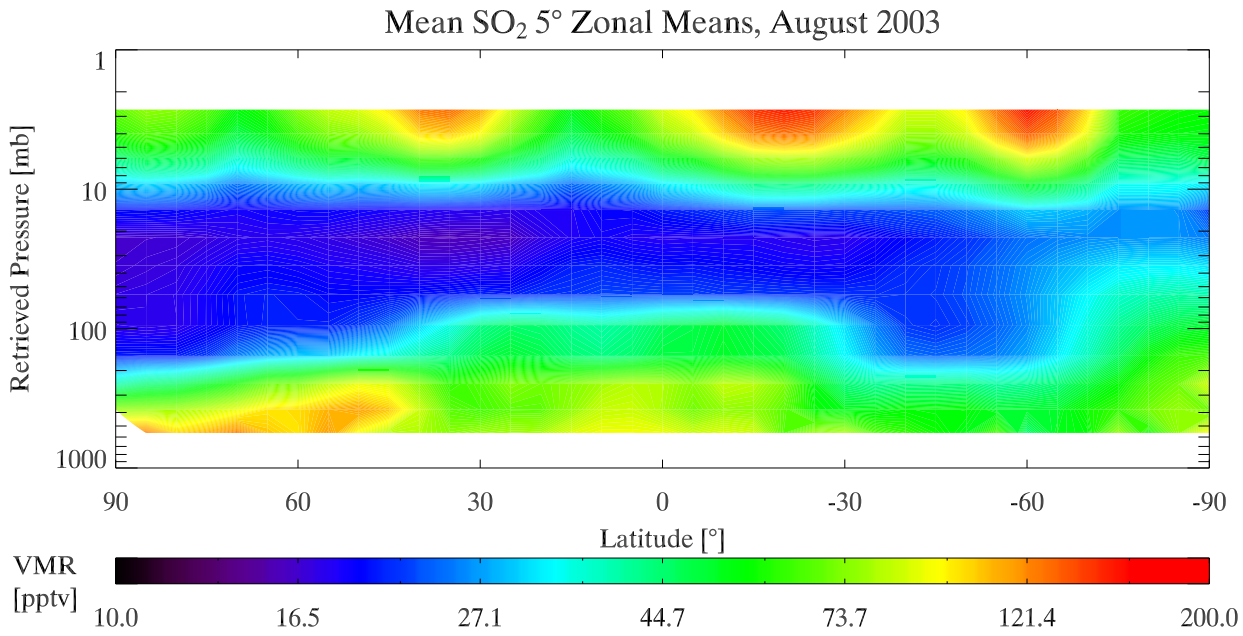

Figure 8. Zonal mean SO_2 distribution, August 2003, displayed in a similar manner to Figure 6. We can see a clear Northern Hemispheric source term that has been assigned to anthropogenic emissions, although the extent to such high latitudes is less certain. The tropopause is distinct as SO_2 has a short lower stratospheric lifetime. The increase above 10 mb, or 30 km, is thought to be due to the photolysis of gas-phase sulphuric acid that has boiled from the top of the stratospheric aerosol layer. The mid-stratosphere values strongly reflect the a priori values as the signal has dropped below the detection threshold for such low VMRs. The enhancement over the South pole is yet to be assigned, and is thought to arise from the low temperatures. However, some mechanisms have been suggested and initial investigations into published results from models have suggested that there is an enhancement in this region (e.g. Liao et al. [12]).

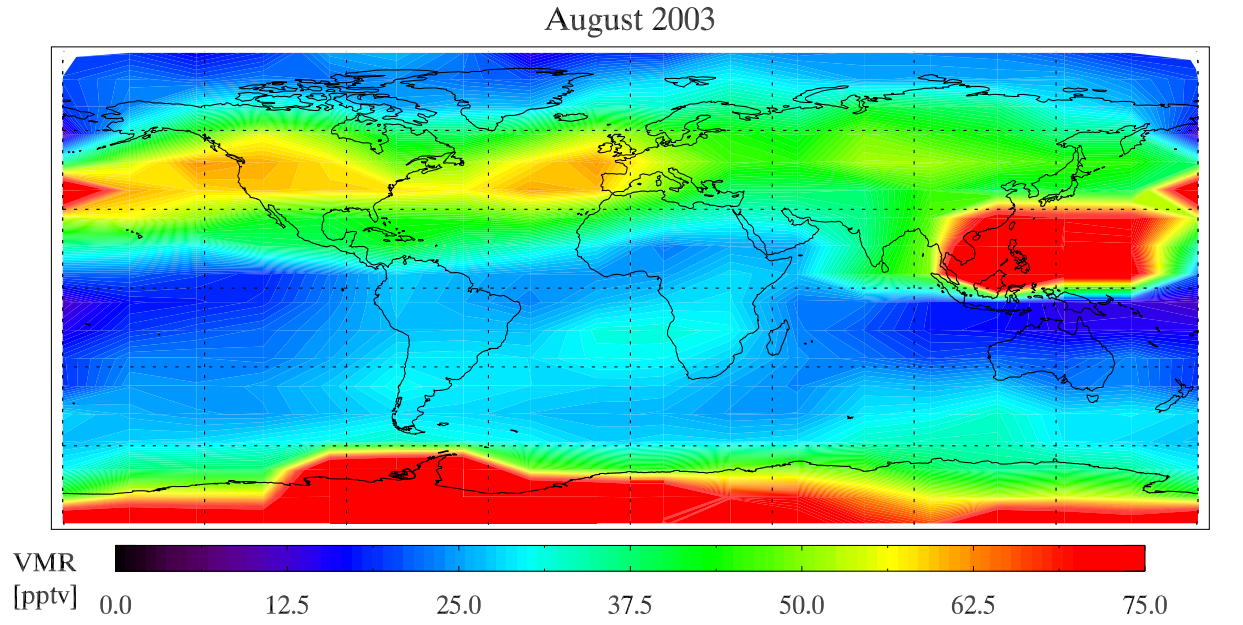

Figure 9. A similar plot to Figure 7, but for SO_2. The Antarctic values seem unreasonably high, as do those over Indonesia – although a proportion may be assigned to deep convective events and biomass burning. The North American and European enhancements are not quite centred on the respective continents, which gives some cause for concern. In addition expected enhancements due to effusive volcanic activity and other industrialised regions such as India have not been observed. However, the interhemispheric variation showing more (anthropogenic) emission in the Northern Hemisphere is directly in line with expectations. As there was no latitudinal variation in the prior information used in the retrieval, this is an encouraging result.

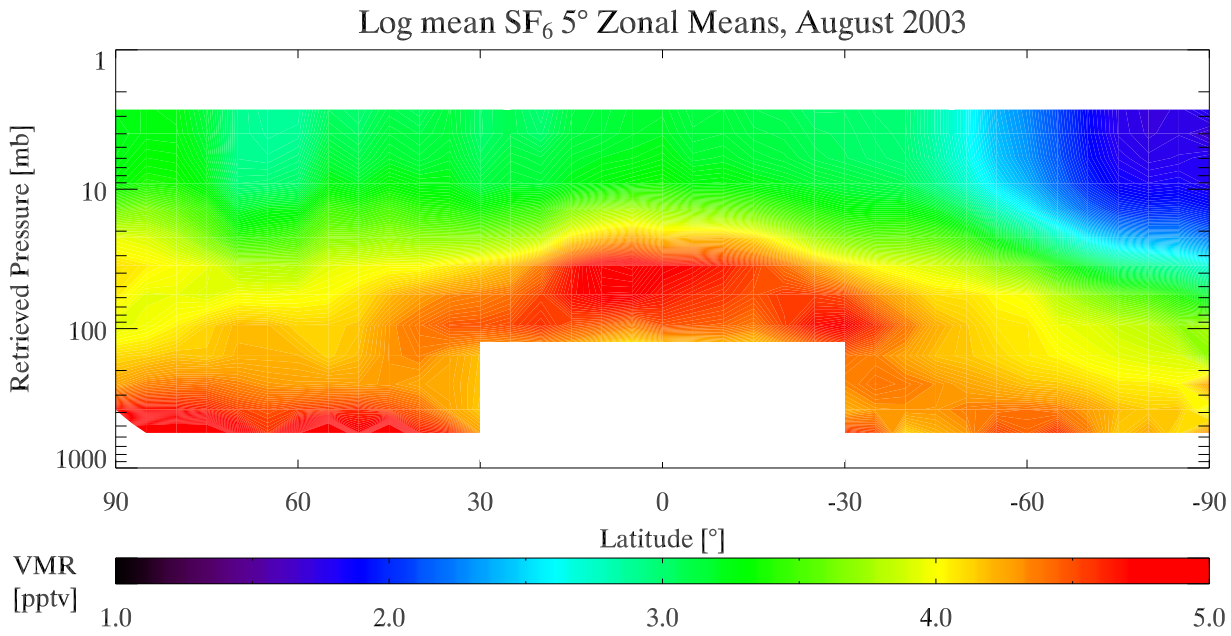

Figure 10. Zonal mean SF_6 distribution, August 2003, displayed in a similar manner to Figure 6. Expected features, such as the low over the Antarctic pole due to the downward motion of air from the mesosphere, and higher Northern Hemispheric values at the lowermost altitudes can be seen. The tropical mid troposphere had been masked in this plot due to cloud issues.

3.1. OCS

One of the first results for OCS, a mean profile, is shown in Figure 5. This result can be compared to the shape of the climatology shown in Figure 1. The lower altitudes are similar in value and contain almost entirely measurement information. Towards the top of the profile, around 35 km, the contribution from the measurement is much reduced. However, the result is still an improvement over the previous data which were purely an extrapolation of the 20 to 25 km values.

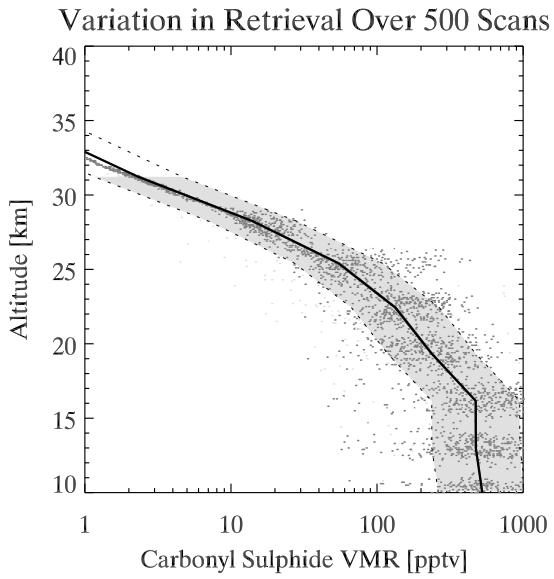

Figure 5. Sample of results from the OCS retrieval, showing the mean retrieved profile, with the standard deviation shown as the shaded region. Points represent the distribution of retrieved values. Some of this scatter arises from variability around the orbits used. The profile reported in Chin & Davis [4] is similar in the lower atmosphere but, probably due to the extrapolation that was performed, reaches 1 pptv at around 37 km instead of 33 km.

Collated global results for OCS are shown in Figures 6 and 7, which contain approximately 10,000 successful profile retrievals over the month of August 2003. This corresponds to around 200 orbits of data, which is just over half the number of orbits performed by the satellite in that period. It is hoped to use the remaining data as it becomes available. Figure 6 shows the zonal mean for a 5° latitude bin size against retrieved pressure, which is the result of the joint pressure and temperature retrieval that is performed before the trace gas retrieval. The key features are described in the figure caption. Figure 7 shows a 'slice' through this zonal mean field to show the global distribution. In this case the third retrieval element in each profile was selected before being binned to the 20° longitude by 10° latitude grid according to the geolocation recorded in the ESA level 1B data product. This element corresponds to profile points whose altitudes lie in the range 11 to 13 km (approximately 150 to 250 mb). Additional zonal mean plots were created to examine the variation within the month, in order to check for internal consistency. The comparison of the first half of the month with the second half showed similar structure. Due to the lifetime and loss mechanisms of OCS, no diurnal variation was expected. The daytime and nighttime zonal means were indeed similar but contained some significant discrepancies. Some originate from the bias in global coverage between day and night, that originates

from an incomplete data set for the month. The remaining differences are under investigation.

3.2. SO_2

The initial results for SO_2 shown in Figures 8 and 9 were constructed in the same manner as for OCS. The figure captions contain a description of the key features along with suggestions as to the origin of some unexpected anomalous features.

The atmospheric extremes in the southern polar region give rise to greater uncertainties and higher variabilities in all the species. Part of the reason for this is the strong reduction in the strength of the thermal emission, on which MIPAS relies, when the temperatures drop below 200 K. In addition there is a highly perturbed chemical environment which is currently only considered as a series of 'polar climatology' profiles. Finally, there exist very high altitude clouds, such as polar stratospheric clouds, which either reduce the number of samples (if detected as cloud and flagged) or subtly perturb the spectrum in ways that our retrieval is unable to accommodate.

3.3. SF_6

Finally, the zonal mean result for SF_6 shown in Figure 10. There is more variability in the field than would be expected from such a long-lived species, although the entire scale covers only 5 pptv. The most interesting feature is the low above the Antarctic polar vortex attributed to descending mesospheric air. The low values at higher altitudes are a mixture of the greater age of air and the first significant SF_6 loss mechanism which occurs in the lower mesosphere. As with all three species, the prior information contains no latitudinal structure, so this 'low' originates entirely from features within the MIPAS spectra.

4. CONCLUSIONS

We have shown the progress that is currently being made in extending the list of species that may be retrieved from MIPAS data. All three species are currently available for August 2003 with information on latitude, longitude and altitude available, allowing both zonal means and global maps to be created. The initial validation work, based on the retrieval diagnostics and literature searches for model and measurement data is encouraging. The fields presented here contain significantly more geolocated measurement data than are available in the literature. As the previously highlighted issues with each of the species – such as the persistent enhancement and low measurement density over Indonesia – are resolved, this work should form the basis of a valuable dataset covering the *measured* 3-dimensional distributions of these species over the globe.

Some provisional work has been performed in applying MIPAS observations to the partitioning and mass budgets of OCS and SO_2 in the upper troposphere and stratosphere, and as more retrieval data becomes available we hope to pursue this area. Indeed, first results indicate that the partitioning of these species given in the 2002 Scientific Assessment of Ozone Depletion is out by 30 to 50%.

5. FURTHER WORK

An assessment of the similarity between the same months in 2002, 2003 and 2004 will contribute towards both the validation and the useful application of MIPAS data. Comparison against model fields would assist validation of the data as will the use of any in situ or alternative colocated measurements. In addition, calculation of OCS and SO_2 fields for the entire year of 2003 would useful from both a validation and an application point of view. Related to this is the investigation of the Southern Hemispheric OCS variability and structure. Other consequences of more accurate abundances and variability are improved estimates of atmospheric lifetimes.

On a more technical side, there remain a variety of subtleties to investigate. Firstly, it is expected to begin the transition to a newer retrieval code, which is able to perform joint retrievals with other species. The second area of investigation is pushing at the cloud boundary, to try and reduce the size of the data 'gaps' around the equator. Finally, as already discussed, investigations into the various anomalies, such as high south polar SO_2, need to be explained.

FURTHER INFORMATION

The Oxford group group performs a variety of trace gas retrievals and MIPAS data health-monitoring. A large amount of diagnostic information together with preliminary information for other months is available from our website, `http://www.atm.ox.ac.uk/group/mipas/`.

ACKNOWLEDGMENTS

We would like to acknowledge NERC (UK) for funding this research and the Royal Meteorological Society for providing travel assistance.

REFERENCES

[1] AMIL2DA, 2003, AMIL2DA Final report, Tech. rep., IMK, co–ordinated by T. von Clarmann

[2] Barnes I., Becker K., Patroescu I., 1994, Geophys. Res. Lett., 2389–2392

[3] Burgess A., Grainger R., Dudhia A., Payne V., Jay V., March 2004, Geophys. Res. Lett., 31, L05112, doi:10.1029/2003GL019143

[4] Chin M., Davis D., 1995, J. Geophys. Res., 100, 8993

[5] Connell P.O., Heil F., Henriot J., et al., 2000, SF_6 in the electric industry, status 2000, www.cigre-sc23.org/SF6/status2000.pdf

[6] Crutzen, 1976, Geophys. Res. Lett, 3, 73

[7] Dudhia A., Jay V., Rodgers C., 2002, Applied Optics, 41, 3665

[8] Harnisch J., Eisenhauer A., July 1998, Geophys. Res. Lett., 25, 2401

[9] Harnisch J., Borchers R., Fabian P., Kourtidis K., 1995, Environ. Sci. Pollut. Res., 2, 161

[10] Kettle A., Kuhn U., von Hobe M., Kesselmeier J., Andreae M., November 2002, J. Geophys. Res.-Atmos., 107, 4642

[11] Ko M., Sze N.D., Wang W.C., et al., 1993, Journal of Geophysical Research, 98, 10499

[12] Liao H., Adams P., Chung S., et al., 2003, J. Geophys. Res., 108(D1), 4001, doi:10.1029/2001JD001260

[13] Maiss M., Brenninkmeijer C., October 1998, Environ. Sci. Technol., 32, 3077

[14] Maiss M., Levin I., April 1994, Geophys. Res. Lett., 21, 569

[15] Maiss M., Steele L., Francey R., et al., May 1996, Atmos. Environ., 30, 1621

[16] Notholt J., Kuang Z., Rinsland C., et al., April 2003, Science, 300, 307

[17] Pitari G., Mancini E., Rizi V., Shindell D., 2002, J. Atm. Sci., 59, 414

[18] Remedios J., 2001, www.atm.ox.ac.uk/RFM/rfm_downloads.html, Downloads of Reference Atmospheres

[19] Rinsland C., andM.C. Abrams M.G., Lowes L., Zander R., Mahieu E., November 1993, J. Geophys. Res.-Atmos., 98, 20491

[20] Rinsland C., Goldman A., Stephen T., et al., April 2003, J. Quant. Spectrosc. Radiat. Transf., 78, 41

[21] Rodgers C., 2000, Inverse Methods for Atmospheric Sounding: Theory and Practice, World Scientific

[22] Seinfeld, Pandis, 1997, Atmospheric Chemistry and Physics: From Air Pollution to Climate Change, Wiley

[23] Spang R., Remedios J., Barkley M., 2004, Adv Space Res, 33, 1041

[24] Timmreck C., November 2001, J. Geophys. Res.-Atmos., 106, 28313

[25] Watts S., 2000, Atmos. Environ., 34, 761

[26] Wayne R., 1999, Chemistry of Atmospheres, 3rd edition, Wiley

[27] Weisenstein D., Yue G., Ko M., et al., June 1997, J. Geophys. Res., 102, 12019

[28] Weiss P., Andrews S., 1995, Geophys. Res. Lett, 22, 215

[29] Zander R., Rinsland C., Demoulin P., August 1991, J. Geophys. Res.-Atmos., 96, 15447

[30] Zepp R., Andrae M., 1994, Geophys. Res. Lett, 21, 2813